https://doi.org/10.5194/egusphere-2026-5987
Preprint. Discussion started: 23 October 2026
© Author(s) 2026. CC BY 4.0 License.

# Active Calcifying Fluid pH Upregulation Facilitates Resilience of the Coral *Tubastraea aurea* to Ocean Acidification

Gowri Krishna Girija[1,2], Li-Chun Tseng[1], Yoshiyuki Iizuka[2], Jiang-Shiou Hwang[1,3*], Yi-Wei Liu[2*]

[1]Institute of Marine Biology, National Taiwan Ocean University, Keelung 202301, Taiwan.
[2]Institute of Earth Science, Academia Sinica, Nangang 11529, Taiwan
[3]Centre of Excellence for the Oceans, National Taiwan Ocean University, Keelung 202301, Taiwan

Correspondence to: Yi-Wei Liu (liuyiwei@earth.sinica.edu.tw), Jiang-Shiou Hwang (jshwang@mail.ntou.edu.tw)

**Abstract.** Ocean acidification poses a critical threat to marine calcifiers, yet the physiological mechanisms allowing certain species to thrive in high-$CO_2$ environments remain poorly understood. Kueishan Island (Taiwan) provides a unique natural laboratory to address this gap. While nearby non-vent reefs support diverse coral communities, the strongly acidified hydrothermal vent fields at Kueishan Island are dominated by the azooxanthellate coral *Tubastraea aurea*. Here, we tested whether this persistence is driven by regulation of the calcifying microenvironment. Using skeletal boron isotope ($\delta^{11}B$) composition and scanning electron microscopy (SEM), we reconstructed calcifying-fluid pH ($pH_{CF}$) and assessed skeletal microstructure in specimens from the vent site (HV, pH ~6.6) and a reference site (FU, pH ~8.0). Despite a ~1.4-unit difference in ambient seawater pH ($pH_{SW}$), the estimated $pH_{CF}$ was indistinguishable between sites (HV $8.45 \pm 0.02$, FU $8.38 \pm 0.01$), resulting in a markedly larger $\Delta pH$ ($pH_{CF} - pH_{SW}$) at the vents. While SEM analysis revealed no gross dissolution at the resolution examined, vent colonies were smaller than reference counterparts, suggesting possible growth constraints under extreme conditions (exploratory given limited colony replication). These findings indicate that *T. aurea* maintains elevated $pH_{CF}$ in exceptionally low-pH seawater, highlighting a physiological capacity that could contribute to skeletal maintenance under future acidified oceans.

## 1 Introduction

Anthropogenic $CO_2$ emissions are driving rapid ocean acidification (OA), fundamentally altering marine ecosystems by reducing the saturation state ($\Omega$) of carbonate minerals required by calcifying organisms (Doney et al., 2009; IPCC, 2023). The vulnerability of reef-building scleractinian corals to this chemical shift is well documented (Anthony et al., 2008; Cornwall et al., 2021); however, the extent to which OA restructures benthic communities by selectively favouring stress-tolerant, non–reef-building taxa remains a critical knowledge gap. Understanding the physiological mechanisms that allow specific dominant species to maintain the calcification-dissolution equilibrium under low-pH conditions is essential for predicting how such mechanisms might reshape community composition as seawater chemistry continues to change (Eyre et al., 2018).

https://doi.org/10.5194/egusphere-2026-5987
Preprint. Discussion started: 23 October 2026
© Author(s) 2026. CC BY 4.0 License.

In scleractinian corals, biomineralization occurs within an extracellular calcifying fluid (CF), semi-isolated between the calicoblastic epithelium and the skeleton (Allison and Finch, 2010; Gagnon, 2013; Tambutté et al., 2011). Many corals elevate calcifying fluid pH ($pH_{CF}$) above ambient seawater pH ($pH_{SW}$), thereby shifting dissolved inorganic carbon speciation toward $CO_3^{2-}$, facilitating aragonite precipitation even when external waters are corrosive (McCulloch et al., 2012a; Wall et al., 2019b, a). However, this capacity varies among species. While many shallow-water zooxanthellate corals exhibit a reduced ΔpH ($pH_{CF} - pH_{SW}$) under stress, deep-sea azooxanthellate corals often maintain strong pH gradients, pointing to distinct physiological strategies for calcification under low carbonate saturation environments (McCulloch et al., 2012b).

This physiological variability raises a concerning possibility for global reef health: that stress-tolerant, azooxanthellate corals may possess a pre-adaptive resilience to ocean acidification, allowing them to functionally replace native reef-builders. Declining aragonite saturation state ($\Omega_{Ar}$) is expected to shift the net balance toward dissolution, driving the loss of three-dimensional reef structure and associated biodiversity (Alvarez-Filip et al., 2009; Fabricius et al., 2011; Hoegh-Guldberg et al., 2007). While many degraded reefs transition toward algal-dominated states (Enochs et al., 2015), an outstanding question is whether stress-tolerant calcifiers can maintain skeletal integrity and occupy ecological space under extreme low-pH conditions, thereby sustaining a calcifying community rather than leaving the reef devoid of coral cover.

The sun coral, *Tubastraea aurea*, is a prime candidate for such successor species. Although some *Tubastraea* species are known as successful marine invaders across the Atlantic and Caribbean via maritime transport (Creed, 2006; Dutra et al., 2023; Lages et al., 2011; Mantelatto and Creed, 2015) – where they often outcompete native benthic taxa through high phenotypic plasticity (Bastos et al., 2024; Tanasovici et al., 2022), the production of allelopathic secondary metabolites (Guilherme da Silva et al., 2022; Iwagawa et al., 2008; Lages et al., 2012), and prolific reproduction even under extreme environments (Bastos et al., 2024; Corrigan et al., 2025) – the genus is native to the Indo-Pacific. Specifically, *T. aurea* occurs naturally along Taiwan's coast, and there is currently no evidence that it behaves as an invasive species or threatens native benthic communities in this region. Therefore, the invasive behaviour documented for other *Tubastraea* species outside their native ranges should not be directly extrapolated to *T. aurea* populations in Taiwan. Instead, understanding the physiological tolerance of this native species remains ecologically relevant, because future ocean acidification could favour stress-tolerant, non-reef-building corals over more sensitive reef-building taxa, potentially altering community composition and reef structural complexity. While sustaining skeletal growth under high-$CO_2$ conditions requires robust physiological control over biomineralization, it remains unknown whether the exceptional resilience of *T. aurea* is driven by the active regulation of its internal calcifying fluid chemistry.

To address this, we leverage Kueishan Island (Taiwan) as a natural laboratory, where shallow-water hydrothermal venting generates persistently low-pH seawater (Chen et al., 2005; Chen et al., 2015; Lin et al., 2019; Mei et al., 2022) and *Tubastraea* dominates the benthic community (Chan et al., 2016). The vent environment represents an extreme acidification regime, with mean seawater pH ($pH_{SW}$) at our hydrothermal vent site (HV) of ~6.6 and transient values as low as ~5.74 previously reported (Girija et al., 2023). These conditions extend far beyond those typically imposed in laboratory ocean acidification experiments (Comeau et al., 2017a; Gagnon et al., 2021) and many natural $CO_2$ seep systems (e.g., the submarine springs investigated by

https://doi.org/10.5194/egusphere-2026-5987
Preprint. Discussion started: 23 October 2026
© Author(s) 2026. CC BY 4.0 License.

Crook et al., (2012) exhibited $pH_{SW}$ values of 6.7–7.9). We acknowledge that shallow-water vents are not perfect analogues for open-ocean OA, as they often involve confounding factors such as temperature, redox chemistry, and localized geochemical heterogeneity (Blain et al., 2021; Hassenrück et al., 2016). Nevertheless, they offer a rare opportunity to assess coral resilience under chronic acidification extremes. In this context, skeletal $\delta^{11}B$ serves as a time-integrated proxy for the pH of the calcifying fluid ($pH_{CF}$) during skeleton formation (Hönisch et al., 2004; McCulloch et al., 2012a; Trotter et al., 2011). Because $\delta^{11}B$ captures the coral's internal chemical environment rather than transient fluctuations in external $pH_{SW}$, it provides a powerful indicator of the coral's physiological capacity to elevate $pH_{CF}$ relative to the acidified ambient background.

We hypothesize that *T. aurea* maintains an elevated $pH_{CF}$ under vent-associated extreme acidity, yielding a large $\Delta pH$ ($pH_{CF} - pH_{SW}$) relative to ambient seawater. To test this, we compared *T. aurea* colonies from the acidic vent site (HV) and a nearby reference site (FU). We applied $\delta^{11}B$ systematics to reconstruct the $pH_{CF}$, coupled with scanning electron microscopy (SEM) to assess skeletal microstructure and dissolution features. We further evaluated whether colony morphology differs between sites as a potential indicator of growth constraint. Together, this study provides the first mechanistic evidence of the physiological strategies that enable *T. aurea* to colonise and persist in seawater conditions that are chemically hostile to most marine calcifiers.

## 2 Methods

### 2.1 Study sites description

Kueishan Island is a volcanic island located off the north-eastern coast of Taiwan. The shallow waters adjacent to its south-eastern coast host numerous hydrothermal vent systems (Zeng et al., 2013). Tectonically, the island is situated approximately 100 km from the Okinawa Trough, at the intersection where Taiwan's fault system meets the trough's southern rifting terminus (Wang et al., 2000).

The hydrothermal effluent in this region exhibits some of the most extreme acidification recorded globally, with pH values dropping as low as 1.52 pH units (Chen et al., 2005). Such conditions strongly restrict the distribution of many calcifying organisms. Previous surveys found that *Tubastraea* first appeared at the outer margin of the peripheral vent zone and became increasingly abundant with distance from the main vent region (Chan et al., 2016). In contrast, our surveys revealed abundant colonies of the azooxanthellate scleractinian coral *T. aurea* (family Dendrophylliidae) growing at approximately 18 m from the nearest identified Yellow Vent mouth. However, because the HV area contains multiple active vent openings, the precise distance between the coral colonies and each individual vent source could not be determined. Previous work characterised the coral habitat as highly acidic, reporting an ambient seawater pH of 5.74 in the vent area (Girija et al., 2023). In contrast, the reference site at Fulong Bay (FU) represent a typical marine pH of ~8.0. Fulong Bay supports abundant populations of *T. aurea* alongside diverse reef-building taxa, providing an ideal environmental baseline for comparing physiological and morphological responses to extreme ocean acidification.

https://doi.org/10.5194/egusphere-2026-5987
Preprint. Discussion started: 23 October 2026
© Author(s) 2026. CC BY 4.0 License.

### 2.2 Sample collection

Coral colonies from the HV and FU sites (n = 3 per site) were collected by SCUBA divers on 1 July 2022. At the HV site, *T. aurea* were collected at a depth of about 18 m. The *T. aurea* population naturally grows in dense clusters separated by <1 m. To minimize the risk of sampling clonal ramets, divers selected spatially distinct colonies; however, given the restricted sampling footprint, colony-level variation at HV is interpreted with caution regarding statistical independence. At the FU reference site, colonies are more widely distributed and were sampled 2–3 m apart from a depth of 10 m. Because site-level replication was limited to three colonies, subsequent statistical comparisons are treated as exploratory. Following collection, colonies were transported to the laboratory in a cooler on ice and stored in -20 $^{o}$C freezer until further processing.

Discrete seawater samples were collected at the HV and FU coral-sampling sites at day 1, 8 and 16 days from coral sampling to characterize local temperature, pH, dissolved oxygen (DO), and salinity conditions. Seawater samples were collected adjacent to the coral habitat in polycarbonate bottles, which were filled completely to minimize headspace and sealed underwater immediately after collection. Upon retrieval of the samples to the surface, seawater parameters were measured promptly on board the vessel using a multiparameter probe (Hanna Instruments Inc., RI, USA). The retrieval time varied depending on prevailing currents and tidal conditions and was not recorded precisely. The stated instrument accuracies were ±0.02 for pH, ±0.15 °C for temperature, ±1.5% of the reading or ±0.10 mg $L^{-1}$ for DO (whichever was greater), and ±2% of the reading or ±0.01 PSU for salinity (whichever was greater) (Girija et al., 2024). Temperatures are reported to one decimal place in accordance with the instrument accuracy.

### 2.3 Preparation for Boron isotope analysis

Soft tissue was removed from the collected coral colonies using an airbrush. The bare skeletons were then treated with $H_2O_2$ (buffered with NaOH to pH > 8) at room temperature for 48 hours to eliminate any residual organic matter. Skeletal powders were obtained by micro-drilling targeted domains using a diamond microdrill: (1) the uppermost thecal margins (representing the newly extending growth front) (hereafter “Cr”; Fig.1), and (2) the coenosteum (hereafter “Cn”; Fig. 1).

https://doi.org/10.5194/egusphere-2026-5987
Preprint. Discussion started: 23 October 2026
© Author(s) 2026. CC BY 4.0 License.

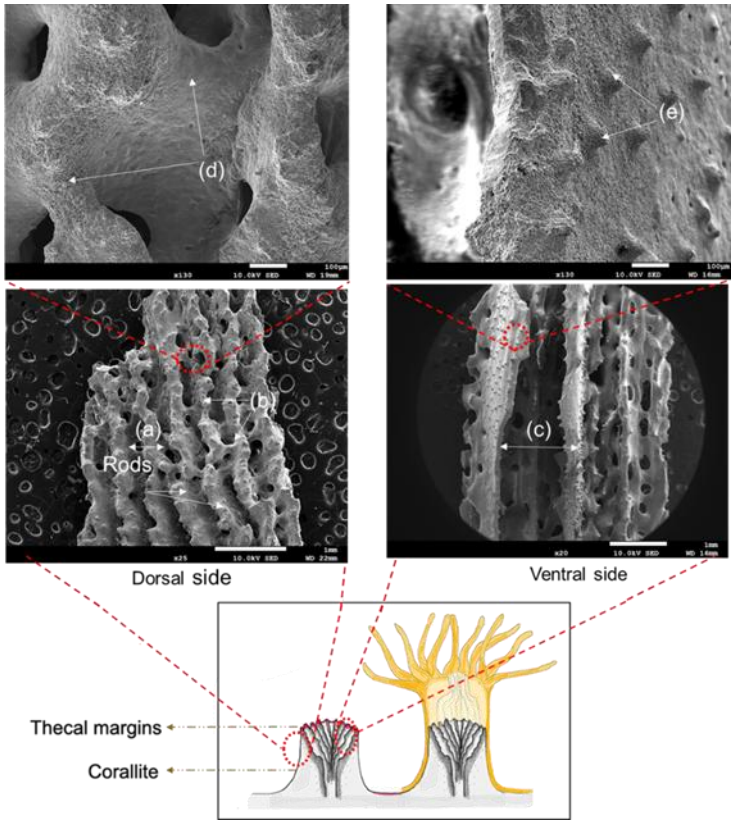



**Figure 1: Schematic illustration of targeted skeletal domains for morphological and isotopic analyses. Morphometric parameters quantified via SEM include: (a) inter-rod distance on the dorsal side of the corallite, (b) perforation diameter on the corallite wall, (c) inter-septa distance on the ventral side, (d) rod thickness on the dorsal side, and (e) septa spine length. The red shaded regions indicate the specific skeletal domains (the uppermost thecal margins and coenosteum) extracted for $\delta^{11}B$ analysis.**

Further processing and boron isotope analysis followed the protocols described by Liu et al., (Liu et al., 2024). To minimize external boron contamination, all subsequent steps were performed in a Class 10,000 cleanroom under a Class 10 laminar flow hood equipped with boron-free ULPA filters at the Institute of Earth Sciences, Academia Sinica (IES). Approximately 2 mg of skeletal powder was transferred to an acid-cleaned polypropylene (PP) centrifuge tube and rinsed three times with Milli-Q water (dispensed from a Milli-Q ADVANTAGE system equipped with a Q-GUARD Boron Pack). The powder was then subjected to a secondary oxidative cleaning overnight using 10% $H_2O_2$ (buffered with NaOH to pH > 8) at room temperature. Following three additional Milli-Q water rinses, the cleaned powder was dried at 60 °C and dissolved in 1.7N HCl to achieve a concentration of ~750 ppb of boron for subsequent purification. All acids and reagents used were of ultrapure laboratory grade.

https://doi.org/10.5194/egusphere-2026-5987
Preprint. Discussion started: 23 October 2026
© Author(s) 2026. CC BY 4.0 License.

### 2.4 Boron isotopic analysis

Boron was purified from the dissolved carbonate samples using a micro-sublimation method. Approximately 50 µL of each sample was pipetted onto the inner cap of a 7 mL conical-bottomed Savillex PFA vial. The vials were tightly sealed, inverted, and heated to 70 °C on a hotplate for 16 hours to allow the sublimated boron to condense in the conical tips. The purified samples were then diluted to a boron concentration of 10 ppb in 0.1 N $HNO_3$ and analyzed using a Neptune Plus MC-ICPMS at IES, following the protocols of Liu et al. (Liu et al., 2018).

A standard-sample-standard bracketing technique was employed to determine the coral $\delta^{11}B$ values, with the inter-laboratory coral standard JCp-1 included to monitor analytical performance. Prior to use, each PFA vial was checked and the total handling blank consistently remained below 75 pg. Analysis of the JCp-1 standard yielded a mean values of 24.24 ± 0.45‰ (2σ, n = 16), which comparable to the established post-cleaning literature values of 24.25 ± 0.22‰ (Gutjahr et al., 2021). Measurements of replicate subsamples confirmed precision and accuracy consistently within the 2σ threshold, ensuring robust and conservative estimates for all subsequent carbonate chemistry calculations.

### 2.5 Calcifying fluid pH calculations

Calcifying-fluid pH ($pH_{CF}$) was estimated from skeletal $\delta^{11}B$ using the established boron isotope pH proxy equation (Eq. 1) (Zeebe and Wolf-Gladrow, 2001).

$$pH_{CF} = pK_B - \log\left(\frac{\delta^{11}B_{SW} - \delta^{11}B_{carbonate}}{\alpha\delta^{11}B_{carbonate} - \delta^{11}B_{SW} + 1000(\alpha - 1)}\right) \quad (1)$$

where $\delta^{11}B_{coral}$ is the measured isotopic composition of the skeleton, and $\delta^{11}B_{SW}$ is the boron isotopic composition of seawater (39.61‰ (Foster et al., 2010)). This seawater value is treated as a constant due to boron's long residence in the global ocean (Lemarchand et al., 2002). The isotopic fractionation factor between aqueous boric acid and the borate ion (α) was set to 1.0272, following Klochko et al. (Klochko et al., 2006). The term $pK_B$ represents the dissociation constant of boron, which was calculated using site-specific temperature and salinity data. Because this $\delta^{11}B$-based $pH_{CF}$ reflects the internal chemistry of the calcifying fluid at the time of skeletal deposition, it provides a quantitative estimate of the coral's physiological capacity to regulate its calcifying microenvironment, rather than acting as a direct proxy for ambient external $pH_{SW}$.

### 2.6 SEM analysis

Following powder extraction for isotopic analysis, the remaining coral skeletons were prepared for SEM. To buffer the skeletal pH and improve structural stability, the samples were immersed in a NaOH solution for 24 hours, subsequently rinsed with Milli-Q water, and air-dried. The skeletons were then sectioned into smaller fragments using a microdrill saw. These fragments were mounted onto stubs using conductive carbon adhesive tape, specifically oriented to allow observation of both dorsal and ventral surfaces of the corallite.

The mounted samples were sputter-coated with platinum and examined using a Field Emission Scanning Electron Microscope (FE-SEM, JEOL JSM-7100F-LV) at the EPMA Laboratory, Institute of Earth Sciences, Academia Sinica. Imaging was

https://doi.org/10.5194/egusphere-2026-5987
Preprint. Discussion started: 23 October 2026
© Author(s) 2026. CC BY 4.0 License.

conducted under high vacuum ($9.6 \times 10^{-5}$ Pa) with an accelerating voltage of 10 kV and a probe current of 0.1 nA. The following morphometric parameters were quantified on the dorsal side: (1) inter-rod distance, (2) perforation diameter, and (3) rod thickness. On the ventral side, we measured: (1) inter-septa distance and (2) spine length (Fig. 1).

### 2.7 Skeletal morphometrics

Of the three colonies collected per site, a subset of two colonies per site was randomly selected for skeletal morphometric analysis. High-resolution images were acquired using a stereo microscope equipped with image capture software to quantify calyx and coenosteum dimensions. Depending on the overall colony size, 8–10 polyps were imaged per colony. Calyx size was measured as surface area ($mm^2$), and coenosteum length was measured in millimetres (mm). Polyp-level measurements were averaged within each colony to obtain colony-level means, which were subsequently treated as independent biological replicates for site-level comparisons. Given the limited colony-level replication (n = 2 per site), statistical comparisons of these colony mean using two-sample t-tests are treated as exploratory and interpreted with cautious.

### 2.8 Statistical Analysis

All statistical analyses were conducted in R (version 4.5.2). Environmental parameters were summarized as site means and treated descriptively due to limited sampling per site. Differences between HV and FU in $\delta^{11}B$ values at the uppermost thecal margins, as well as the corresponding $pH_{CF}$ and $\Delta pH$ values derived from them, were evaluated using two-sided permutation tests (10,000 permutations), generating empirical p-values from randomized reassignment of site labels. To better quantify the magnitude and uncertainty of observed differences, effect sizes (mean differences between sites) and their 95% confidence intervals were estimated using bootstrap resampling (10,000 iterations).

Where multiple skeletal measurements were obtained from the same colony, values were averaged prior to site comparisons to preserve statistical independence and reduce pseudo replication. Quantitative skeletal microstructural features and colony morphometrics were compared using independent-samples t-tests; however, given the small sample sizes and multiple measured variables, these analyses are interpreted as exploratory. Throughout the study, we emphasize effect sizes and uncertainty estimate alongside permutation-derived p-values, and interpret results conservatively in light of our sampling limitations.

## 3 Results

### 3.1 Environmental parameters differed between sites

Hydrographic conditions measured at HV and FU on three discrete sampling occasions spanning 16 days are presented in Table 1. At HV, $pH_{SW}$ ranged from 6.49 to 6.76, with a descriptive mean of 6.61, whereas FU values ranged from 7.96 to 8.07, with a mean of 8.00. Temperature ranged from 27.1 to 27.9 °C at HV and from 27.4 to 29.8 °C at FU, corresponding to

https://doi.org/10.5194/egusphere-2026-5987
Preprint. Discussion started: 23 October 2026
© Author(s) 2026. CC BY 4.0 License.

descriptive means of 27.4 and 29.0 °C, respectively. Salinity varied only slightly (HV: 32.77–33.35 PSU; FU: 32.63–33.16 PSU), while DO range from 4.77 to 4.97 mg $L^{-1}$ at HV and from 5.01 to 6.13 mg $L^{-1}$ at FU (Table 1).

**Table 1 Hydrographic parameters, samples from hydrothermal vent (HV) site and Fulong (FU) site. Temp = temperature, DO = dissolved Oxygen, SD = standard deviation.**

| *Site* | *Timing* | *$pH_{SW}$* | *Temp (°C)* | *Salinity (PSU)* | *DO (mg $L^{-1}$)* |
|---|---|---|---|---|---|
| *HV* | Concurrent with coral collection | 6.76 | 27.2 | 33.35 | 4.77 |
| *HV* | 8 days after initial sampling | 6.49 | 27.9 | 32.99 | 4.8 |
| *HV* | 16 days after initial sampling | 6.6 | 27.1 | 32.77 | 4.97 |
| ***HV*** | **mean ± SD** | **6.62 ± 0.14** | **27.4 ± 0.4** | **33.04 ± 0.29** | **4.85 ± 0.11** |
| *FU* | Concurrent with coral collection | 8.07 | 29.8 | 33.16 | 5.53 |
| *FU* | 8 days after initial sampling | 7.96 | 27.4 | 32.64 | 6.13 |
| *FU* | 16 days after initial sampling | 7.96 | 29.8 | 32.63 | 5.01 |
| ***FU*** | **mean ± SD** | **8.00 ± 0.06** | **29.0 ± 1.4** | **32.81 ± 0.30** | **5.56 ± 0.56** |

### 3.2 Boron isotopes ($\delta^{11}B$) and calcifying fluid pH ($pH_{CF}$)

Skeletal boron isotope composition ($\delta^{11}B$) differed in variability among sampled skeletal domains. Samples taken from the coenosteum (Cn) showed higher dispersion (HV: ±0.6; FU: ±0.81) than the uppermost thecal margins samples (Cr) (HV: ±0.3; FU: ±0.12) (Fig. 2), consistent with greater microstructural heterogeneity and/or time-averaging in non-apical skeletal material. We therefore focus subsequent site comparisons on Cr $\delta^{11}B$ values. Mean Cr $\delta^{11}B$ was 23.56 ± 0.30‰ at HV and 22.81 ± 0.12‰ at FU (Fig. 3A). A permutation test indicated that this difference did not reach the conventional 0.05 significance threshold ($p > 0.05$).

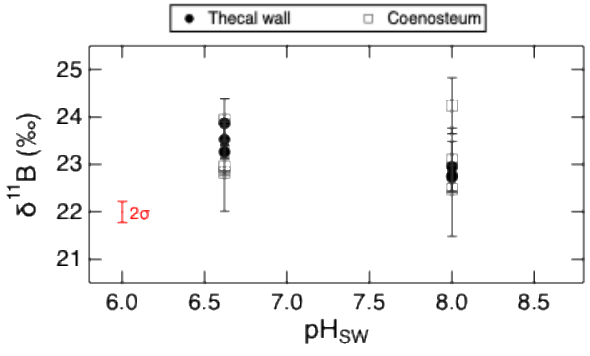



**Figure 2: Skeletal $\delta^{11}B$ values of *Tubastraea aurea* from the hydrothermal vent (HV) (left) and Fulong (FU) (right) sites. Solid circles represent data from the uppermost thecal margins, and open squares represent values from the coenosteum. Sites are distinguished by the seawater pH ($pH_{SW}$) values. Error bars represent ± 2SD of the measurements.**

Using Cr $\delta^{11}B$ to estimate calcifying-fluid pH ($pH_{CF}$), we incorporated site-specific temperature and salinity into the calculation of the boron isotope fractionation constant ($pK_B$). The resulting $pH_{CF}$ was slightly higher at HV (8.45 ± 0.02) than at FU (8.38 ± 0.01) (Fig. 2B). (Fig. 3B). Although the permutation test returned $p = 0.10$, the estimated effect size was 0.07 with a

https://doi.org/10.5194/egusphere-2026-5987
Preprint. Discussion started: 23 October 2026
© Author(s) 2026. CC BY 4.0 License.

210 95% confidence interval of [0.04, 0.09] (Supplementary Table 2), indicating that $pH_{CF}$ remained high and differed only modestly between environments despite large differences in ambient $pH_{SW}$. The pH gradient between calcifying fluid and seawater ($\Delta pH = pH_{CF} - pH_{SW}$) was much larger at the vent site (HV: $1.83 \pm 0.15$) than at the reference site (FU: $0.38 \pm 0.07$) (Fig. 3C), reflecting the extreme external acidity at HV. While the permutation test again yielded $p = 0.10$, the effect size for ΔpH was large (1.45; 95% confidence interval [1.26, 1.63]; Supplementary Table 2). Together, these results show that
215 estimated $pH_{CF}$ remained elevated at both sites, producing a markedly larger ΔpH under vent-associated low pH conditions.

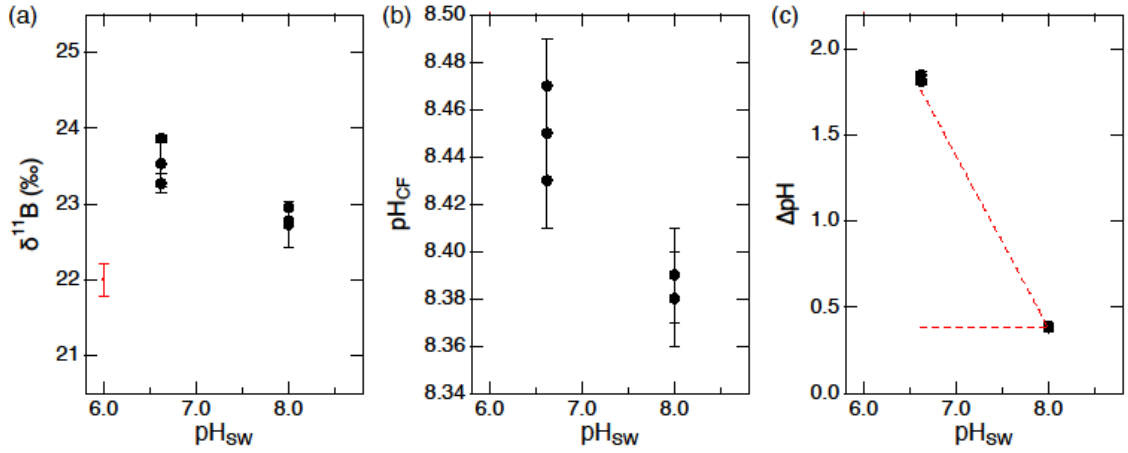



**Figure 3: Boron isotopic composition and inferred calcifying-fluid pH at the uppermost thecal margins of *Tubastraea aurea*. Scatterplots showing: (a) skeletal δ¹¹B values of coral samples collected across the two environmental pH conditions, (b) calcifying**
220 **fluid pH derived from the skeletal δ¹¹B values, and (c) the pH offset (ΔpH) between the calcifying fluid and ambient seawater ($\Delta pH = pH_{CF} - pH_{SW}$). Error bars represent ± 2SD of the analytical measurements or the propagated ± 2SD of the calculated results (panels b and c). Red dashed lines represent theoretical reference lines indicating either no pH regulation ($pH_{CF} = pH_{SW}$) or a constant magnitude of pH-regulation (where $pH_{CF}$ exceeds $pH_{SW}$ by a fixed value).**

### 3.3 Skeletal microstructure

225 Scanning electron microscopy (SEM) of dorsal and ventral corallite surfaces revealed no obvious dissolution textures or gross microstructural degradation in specimens from either site (Fig. 4). Quantitative measurements of corallite skeletal features were broadly similar between sites (Fig. 4; Supplementary Table 3), with the exception of the spacing between vertical rods on the dorsal surface, which differed between sites ($p < 0.05$). Given multiple measured features, this isolated difference is interpreted cautiously and does not indicate a consistent site-wide pattern of skeletal alteration.

https://doi.org/10.5194/egusphere-2026-5987
Preprint. Discussion started: 23 October 2026
© Author(s) 2026. CC BY 4.0 License.

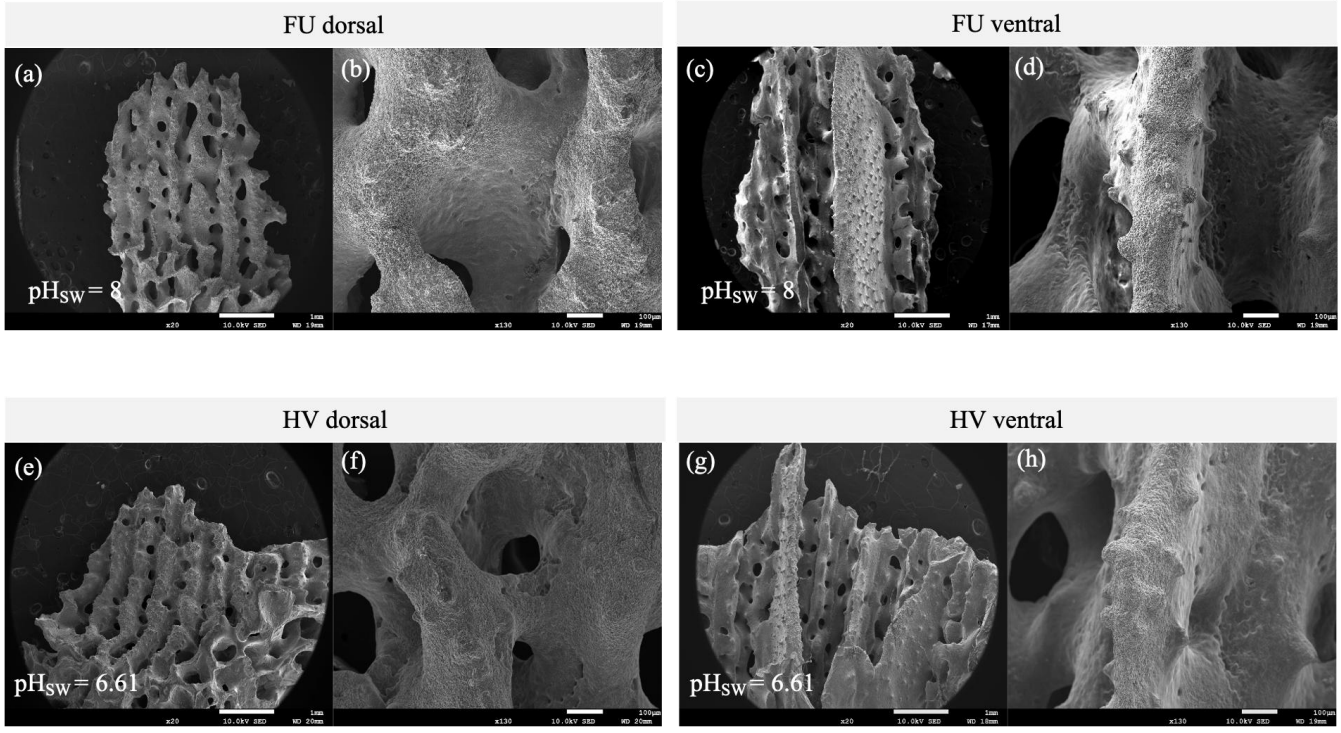



**Figure 4: Scanning electron microscope (SEM) images of *Tubastraea aurea* skeletal ultrastructure. Representative images from the Fulong reference site (FU; a-d) and the hydrothermal vent site (HV; e-h). Images depict the dorsal surface of the corallite at 20× (a, e) and 130× (b, f) magnification. The ventral surfaces, illustrating the septa, is shown at 20× (c, g) and at 130× (d, h), with the higher magnification highlighting the presence of distinct spines. Scale bars: 1mm in (a), (c), (e) and (g); 100 µm in (b), (d), (f) and (h).**

### 3.4 Colony morphometrics

Colonies collected from the FU site were larger than those from the HV site (FU: 13.0 ± 2.83 cm, n = 2; HV: 3.5 ± 0.71 cm, n = 2; Supplementary Table 4). Because colony-level replication was limited, statistical tests on colony means are interpreted as exploratory. Nevertheless, colony morphology differed consistently between environments: HV colonies exhibited tightly packed corallites with minimal to absent coenosteum (Supplementary Fig. 1), whereas FU colonies displayed corallites separated by well-developed coenosteum, particularly in older growth regions. Consistent with these qualitative observations, coenosteum length was markedly greater at the FU site (24.98 ± 1.66 mm) than at the HV site (7.07 ± 1.10 mm; exploratory t-test, $p$ = 0.01). In contrast, calyx area and perimeter length showed overlapping values between sites and did not exhibit a consistent site-level pattern (Supplementary Table 4).

https://doi.org/10.5194/egusphere-2026-5987
Preprint. Discussion started: 23 October 2026
© Author(s) 2026. CC BY 4.0 License.

## 4 Discussion

### 4.1 Active pH regulation overrides passive diffusion

A central finding of this study is the capacity of *T. aurea* to maintain an elevated $pH_{CF}$ despite a ~1.4-unit disparity in ambient seawater pH. Although discrete water data suggest a relative short-term water condition at both sampling sites, historical data from the area confirm a more chronic low pH condition at the vent site (Lin et al., 2019; Mei et al., 2022). In this context, $\delta^{11}B$-derived estimates indicate a $pH_{CF}$ of ~8.45 at HV and ~8.38 at FU (Table S1; Fig. 3B). Although this corresponds to a modest site difference in $pH_{CF}$ (effect size ~0.066; 95% CI ~0.042–0.089; permutation $p \approx 0.10$), the data clearly demonstrate that the internal $pH_{CF}$ remains heavily buffered against external $pH_{SW}$ extremes (Guillermic et al., 2021; Kubota et al., 2017). Regulating $pH_{CF}$ is essential for sustaining aragonite precipitation and efficient calcification (Comeau et al., 2017a; Venn et al., 2011). Consequently, the pH gradient between calcifying fluid and seawater ($\Delta pH = pH_{CF} - pH_{SW}$) is substantially larger at the vent site (Table S1; Fig. 3C), reflecting the organism's ability to sustain a highly elevated internal pH against an exceptionally steep external gradient a response consistent with previous observations in stress-tolerant corals (Kubota et al., 2017; McCulloch et al., 2012a).

The measured skeletal $\delta^{11}B$ values were consistently higher than those predicted from the theoretical $\delta^{11}B$–pH relationship using the measured ambient seawater pH. At a seawater pH of ~6.5, the theoretical $\delta^{11}B$–pH relationship predicts a $\delta^{11}B$ of ~12.18‰ (Eq (1)), yet corals from HV exhibited a mean skeletal $\delta^{11}B$ value of 23.56‰. Under the conventional borate–pH framework, this approximately 10.5‰ offset corresponds to a $\delta^{11}B$-derived $pH_{CF}$ estimates. This discrepancy likely arises because coral biomineralization spans multiple distinct phases or compartment with differing chemical compositions specifically, intracellular vesicles carrying amorphous carrying amorphous calcium carbonate (ACC) precursors, and the extracellular fluid where crystalline aragonite ultimate form (Allison et al., 2023). Furthermore, trace element modelling suggests that the transformation of ACC into crystalline aragonite may involve the full dissolution of these precursors followed by re-precipitation (Foster and Evans, 2026). Because these compartments possess differing chemical compositions and precipitation dynamics, our primary interest lies in the organism's ability to maintain overall skeletal integrity. Consequently, we argue that the skeletal $\delta^{11}B$ value should not be viewed merely as a snapshot of a single fluid compartment's pH. Instead, it serves as a time-integrated proxy that captures the net chemical outcome of these combined biomineralization pathways. By recording the integrated signal of these processes, $\delta^{11}B$ provides a superior metric for assessing how the coral successfully manipulates its internal conditions to precipitate a thick, structurally sound skeleton under extreme external acidity.

Under this context, we found the inter-site $\delta^{11}B$ offset was ~0.74‰, and with a descriptively higher mean value at the lower-pH HV site, in direct contrast to earlier studies that reported declining $\delta^{11}B$ with decreasing $pH_{SW}$ in cold-water and other shallow-water corals (Krief et al., 2010; McCulloch et al., 2012b; Tanaka et al., 2015). This reversal of the expected trend further supports that *T. aurea* increases its upregulation capacity under more acidic conditions rather than allowing $pH_{CF}$ to track external pH.

https://doi.org/10.5194/egusphere-2026-5987
Preprint. Discussion started: 23 October 2026
© Author(s) 2026. CC BY 4.0 License.

An alternative explanation for the observed $\delta^{11}B$ offsets could involve kinetic effects or dissolved inorganic carbon (DIC)-driven changes in the ratio of boric acid diffusion and seawater exchange ($D_B/k_z$), rather than enhanced physiological regulation. As Gagnon et al., (2021) demonstrated, the isotopic composition of the calcifying fluid is highly sensitive to the balance between bulk seawater flushing ($k_z$) and neutral boric acid diffusing across the tissue membrane ($D_B$). Because boric acid is isotopically heavy, this diffusion acts as a pump that artificially elevates the $\delta^{11}B$ of the calcifying fluid. In their model, elevated DIC fuels faster precipitation, which dilutes this slow diffusion pump with bulk seawater. This theoretically results in lower $\delta^{11}B$ values, even if the true $pH_{CF}$ remains completely constant. In the present study, average DIC levels were ~2177 µmol $kg^{-1}$ at HV (Lin et al., 2019) and ~1904 µmol $kg^{-1}$ at FU (Jiang et al., 2011). According to this model, the DIC difference between sites would produce only a ~0.2‰ lower $\delta^{11}B$ at HV a difference unresolvable at current analytical precision and far too small to account for the observed patterns. Crucially, the theoretical kinetic effect of the vent's higher DIC would be to decrease the skeletal $\delta^{11}B$; instead, we observe even slightly higher $\delta^{11}B$ values at HV. The massive discrepancy between the acidic external $pH_{SW}$ at HV and the persistently high inferred $pH_{CF}$ far exceeds the modest offsets expected from DIC variations or diffusion effects alone. The lower $\delta^{11}B$ values of *T. aurea* relative to other azooxanthellate corals therefore more likely reflect species-specific differences in calcification dynamics such as differing $D_B/k_z$ ratios rather than a lack of physiological regulation, highlighting that azooxanthellate corals do not represent a uniform functional group.

Coupled with the absence of obvious microscopic dissolution textures in our SEM observations (Fig. 4), these results indicate that *T. aurea* successfully sustains a highly regulated calcifying environment under vent-associated extreme acidity. Because we did not directly quantify calcification rates or energetic costs, we conservatively interpret these findings as evidence of the physiological capacity to regulate $pH_{CF}$ and preserve skeletal integrity, rather than as definitive proof of unimpaired overall calcification performance. Ultimately, these results underscore the necessity of species-specific assessments when interpreting $\delta^{11}B$-derived $pH_{CF}$ across diverse coral life histories and habitats.

### 4.2 Skeletal heterogeneity and reliability of the proxy

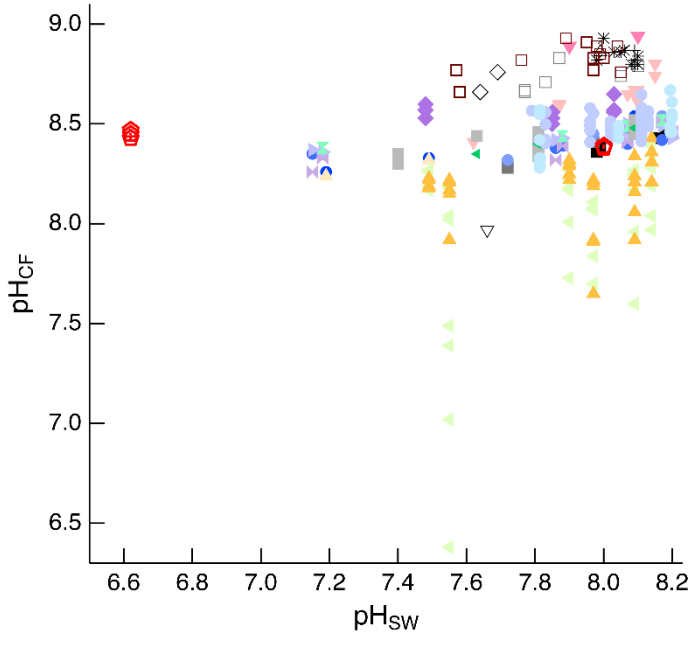
Our $\delta^{11}B$ measurements exhibited differing variance among sampled skeletal domains, with greater variability in coenosarc-associated material than in the uppermost thecal margins (Fig. 2). Such spatial heterogeneity is well documented in scleractinian corals and is generally attributed to biologically mediated differences in calcification processes rather than direct control by ambient seawater pH (Blamart et al., 2007; Chalk et al., 2021; Holcomb et al., 2014). Previous studies have shown that $\delta^{11}B$ varies across skeletal microstructures and thickening layers due to differences in growth timing, microenvironments, and crystal fabrics. For instance, isotopic contrasts between the Early Mineralization Zone and fibrous aragonite in *Lophelia pertusa* have been linked to distinct growth mechanisms and internal fractionation effects (Blamart et al., 2007), while *Stylophora pistillata* exhibits higher $\delta^{11}B$ sensitivity in lateral skeletal regions compared to apical tips, suggesting reduced isolation of the calcifying fluid from ambient seawater outside the primary growth axis (Holcomb et al., 2014). Similarly, high-resolution 2D $\delta^{11}B$ mapping in *Siderastrea siderea* demonstrates isotopic differences between porous skeletal domains (e.g., columella) and denser thecal walls, reflecting spatially heterogeneous carbonate microenvironments (Chalk et al., 2021).In

https://doi.org/10.5194/egusphere-2026-5987
Preprint. Discussion started: 23 October 2026
© Author(s) 2026. CC BY 4.0 License.

contrast, the uppermost thecal margins represent a spatially constrained, newly extending growth domain, comparable to the "apical tips" highlighted by Holcomb et al., (2014) as locations that can better capture contemporaneous calcifying-fluid chemistry. In this study, the elevated $\delta^{11}B$ variability observed in the coenosteum of *T. aurea* (Fig. 2) is consistent with previous findings. The coenosteum likely represents a zone of skeletal mixing across microenvironmentally distinct growth domains, whereas the uppermost thecal margins preserve a more uniform calcification signal. Accordingly, we exclude coenosteum data and focus on thecal margins for site-level comparisons, ensuring that reconstructed $pH_{CF}$ values reflect physiological regulation at the primary growth front while minimizing microdomain mixing and time-averaging effects inherent to more heterogeneous skeletal regions.

### 4.3 Global context of $pH_{CF}$ regulation in *Tubastraea aurea*

Contextualizing our $pH_{CF}$ estimates within published $\delta^{11}B$ datasets suggests that *T. aurea* exhibits a high capacity for pH up-regulation relative to many shallow-water, reef-building corals (Figs. 5–6). *T. aurea* maintained comparatively higher $pH_{CF}$ values than zooxanthellate corals, but lower than other azooxanthellate species, under both normal and extremely low seawater conditions. While several reef taxa show a reduced ΔpH under acidification stress, certain azooxanthellate and deep-sea species maintain a robust ΔpH across low-Ω environments (McCulloch et al., 2012b), and our results indicate that *T. aurea* aligns closely with these stress-tolerant strategies, characterized by sustained internal pH elevation.




**Zooxanthellate**

| | |
|---|---|
| *Acropora* sp. | (Reynaud *et al.*, 2004) |
| *Acropora digitifera* | (Tanaka *et al.*, 2015) |
| *Acropora nobilis* | (Honisch *et al.*, 2004) |
| *Cladocora caespitosa* | (Trotter *et al.*, 2011) |
| *Cladocora caespitosa* | (Reynaud *et al.*, 2008) |
| *Oculina arbuscula* | (Liu *et al.*, 2020) |
| *Pocillopora damicornis* | (Comeau *et al.*, 2017) |
| *Pocillopora damicornis* | (Guillermic *et al.*, 2021) |
| *Porites* sp. | (Krief *et al.*, 2010) |
| *Porites* sp. | (Allison *et al.*, 2021) |
| *Porites astreoides* | (Eagle *et al.*, 2022) |
| *Porites cylindrica* | (Honisch *et al.*, 2004) |
| *Porites cylindrica* | (Georgiou *et al.*, 2015) |
| *Pseudodiploria strigosa* | (Eagle *et al.*, 2022) |
| *Siderastrea siderea* | (Eagle *et al.*, 2022) |
| *Stylophora pistillata* | (Krief *et al.*, 2010) |
| *Stylophora pistillata* | (Guillermic *et al.*, 2021) |
| *Undaria tenuifolia* | (Eagle *et al.*, 2022) |

**Azooxanthellate**

| | |
|---|---|
| *Caryophyllia smithii* | (McCulloch *et al.*, 2012b) |
| *Corallium* sp. | (McCulloch *et al.*, 2012b) |
| *Desmophyllum dianthus* | (Anagnostou *et al.*, 2012) |
| *Desmophyllum dianthus* | (McCulloch *et al.*, 2012b) |
| *Enallopsammia rostrata* | (McCulloch *et al.*, 2012b) |
| *Lophelia pertusa* | (McCulloch *et al.*, 2012b) |
| *Madrepora oculata* | (McCulloch *et al.*, 2012b) |
| *Tubastraea aurea* | (This study) |

https://doi.org/10.5194/egusphere-2026-5987
Preprint. Discussion started: 23 October 2026
© Author(s) 2026. CC BY 4.0 License.

**Figure 5: Comparison of $pH_{CF}$ in *T. aurea* with previously reported values for other zooxanthellate and azooxanthellate corals (Allison et al., 2021; Anagnostou et al., 2012; Comeau et al., 2017a; Eagle et al., 2022; Georgiou et al., 2015; Guillermic et al., 2021; Hönisch et al., 2004; Krief et al., 2010; Liu et al., 2020; McCulloch et al., 2012b; Reynaud et al. 2008; Reynaud et al., 2004; Tanaka et al., 2015; Trotter et al., 2011). Filled symbols represent zooxanthellate species, whereas unfilled symbols represent azooxanthellate species.**

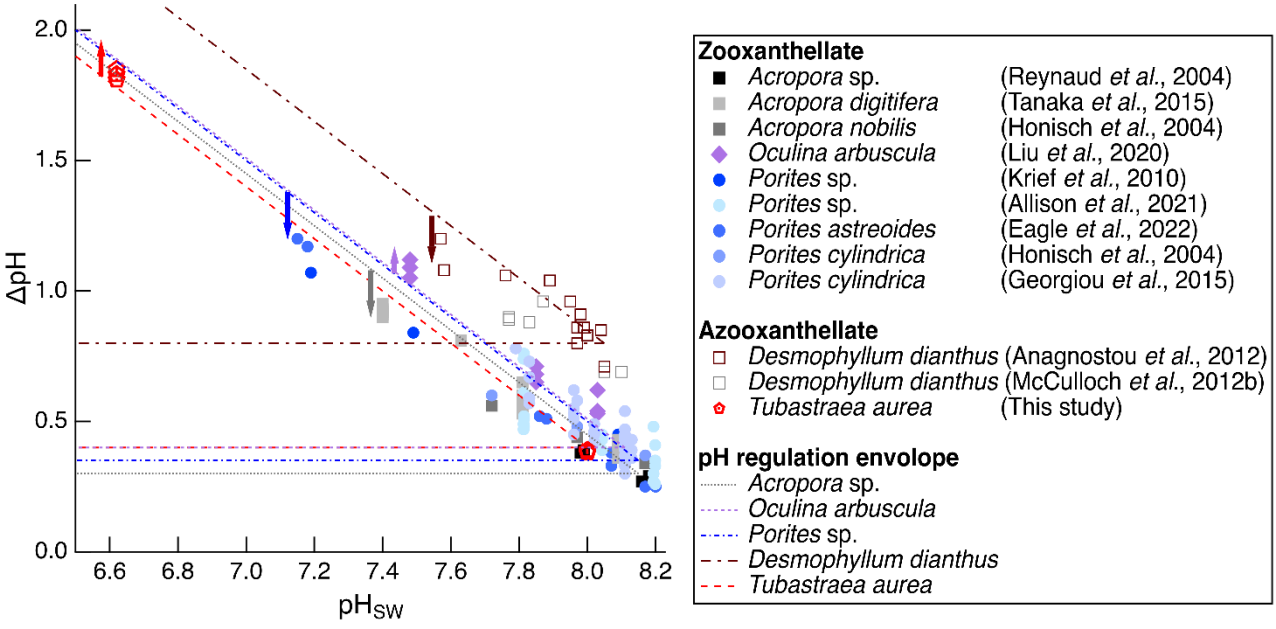



**Figure 6: Comparison of ΔpH in *T. aurea* with previously reported values for other zooxanthellate and azooxanthellate corals (Allison et al., 2021; Anagnostou et al., 2012; Eagle et al., 2022; Georgiou et al., 2015; Hönisch et al., 2004; Krief et al., 2010; Liu et al., 2020; McCulloch et al., 2012b; Reynaud et al., 2004; Tanaka et al., 2015). Filled symbols represent zooxanthellate species, whereas unfilled symbols represent azooxanthellate species. Dash lines show references line of no pH regulation or constant pH regulation of the species.**

To further evaluate this capacity, we assessed how ΔpH in *T. aurea* responds to declining $pH_{SW}$ relative to other taxa (Fig. 6). The upper limit of the ΔpH–$pH_{SW}$ envelope corresponds to a 1:1 ratio between ΔpH and $pH_{SW}$, meaning that species positioned along this boundary sustain a stable $pH_{CF}$ even as surrounding $pH_{SW}$ decreases (Liu et al., 2020). The variation of ΔpH with changing $pH_{SW}$ between our two sites places *T. aurea* near this upper boundary, revealing a stronger capacity to upregulate $pH_{CF}$ even at extremely low $pH_{SW}$ compared with most other zooxanthellate and azooxanthellate corals examined in the literature. Sustaining such a high ΔpH under ocean acidification conditions is essential for coral calcification, though this process demands substantial energy (Allison and Finch, 2010; McCulloch et al., 2012a). To counteract the dissolution risk posed by the extremely acidic conditions at HV, *T. aurea* likely invests considerably more energy in maintaining a high ΔpH (Kubota et al., 2017; McCulloch et al., 2012b), potentially at the expense of other physiological processes, a trade-off explored further in Section 4.4.

Because these comparative plots compile studies utilizing diverse sampling domains, analytical approaches, and environmental contexts, we treat these overarching patterns as contextual rather than definitive meta-analytic inferences. Even so, the

https://doi.org/10.5194/egusphere-2026-5987
Preprint. Discussion started: 23 October 2026
© Author(s) 2026. CC BY 4.0 License.

combination of an exceptionally low external $pH_{SW}$ at HV and a persistently high inferred $pH_{CF}$ highlights the broad physiological range over which *T. aurea* can successfully maintain its calcifying-fluid chemistry.

### 4.4 Potential Trade-offs of pH Homeostasis

Although SEM did not reveal obvious dissolution features in the vent-site skeleton (Fig. 4), colonies from HV were significantly smaller and exhibited reduced coenosteum development between corallites relative to FU colonies, with no significant differences in calyx size (Supplementary Fig. 1; Supplementary Table 3). This pattern contrasts with findings in *Porites*, where increased acidification was associated with a reduction in calyx size accompanied by an increase in coenosteum length as a compensatory response(Allison et al., 2022), but aligns more closely with observations in *S. pistillata*, where reduced coenosteum without significant calyx change was reported under low $pH_{SW}$ (Scucchia et al., 2021). A reduction in colony size along with a decreased polyp-to-coenosarc ratio may represent a morphological adaptation that helps corals minimize maintenance costs (Lasker, 1981), particularly under conditions of extremely low seawater $pH_{SW}$ where substantial energy is required to maintain the balance between calcification and dissolution. While limited colony-level replication requires these morphometric differences to be treated as exploratory, their consistency across sampled colonies suggests a plausible link between extreme environmental stress and altered growth form.

One hypothesis is an energetic allocation trade-off: maintaining a high ΔpH against a steep external gradient is a highly energy-demanding process (Gagnon et al., 2021; Wall et al., 2019a) that likely incurs significant metabolic costs, potentially diverting energy away from skeletal extension and tissue expansion (Roik et al., 2024), and reducing resources available for other metabolic processes potentially leading to slower growth rates (Ross et al., 2017). As an obligate heterotroph, *T. aurea* relies on particle capture (e.g., bacteria, phytoplankton, and zooplankton) to meet energetic demands (Houlbrèque et al., 2004; Kitahara et al., 2020). At HV specifically, populations appear to depend primarily on marine snow (Jeng et al., 2004) and chemosynthetic bacterial associates (Girija et al., 2023) as energy sources, resulting in inherently constrained energy availability. Despite these limitations, *T. aurea* maintains calcification and skeletal integrity within this extreme environment, suggesting that the reduced colony size observed at HV may represent an adaptive resilience strategy in which energetic resources that would otherwise support colony and coenosteum expansion are instead redirected toward maintaining $pH_{CF}$ homeostasis under prolonged exposure to extreme acidity.

In hydrothermal settings, additional physicochemical stressors including variable temperature, reduced oxygen, and vent-derived chemical constituents could further influence both prey availability and basal metabolic costs, compounding these energetic constraints. Although the same species, *T. aurea*, was examined at both sites, our comparison of a single vent-influenced population with a single reference population does not allow the influence of seawater pH to be separated from other site-specific environmental conditions. Nevertheless, the Kueishan Island vent system provides a crucial natural window into how benthic communities might reorganized under severe, chronic ocean acidification. While *T. aurea* is a natural, native component of the benthic community at Kueishan Island rather than an invasive arrival to the vent system, the strong

https://doi.org/10.5194/egusphere-2026-5987
Preprint. Discussion started: 23 October 2026
© Author(s) 2026. CC BY 4.0 License.

physiological resilience demonstrated here sheds light on its broader success as a global opportunist. The energetic capacity to rigorously maintain calcifying fluid homeostasis under extreme chemical stress is a distinct survival advantage. Comparative studies across additional populations, acidified environments, and controlled experimental conditions will be necessary to determine how broadly the physiological responses observed here apply. We emphasize that these mechanisms remain untested in the present study. Future work should aim to quantify: (1) net calcification and skeletal extension rates; (2) respiration and comprehensive energy budgets across vent gradients; (3) feeding rates and prey availability; and (4) the expression or activity of ion-transport pathways involved in proton removal and carbonate chemistry regulation. Furthermore, microbial associates may influence holobiont energetics; prior studies report distinct bacterial communities associated with *Tubastraea* spp., including cyanobacteria in some contexts (Girija et al., 2023, 2024), which could contribute to nutrient cycling and provide metabolic subsidies (Benavides et al., 2017; Lesser et al., 2007). Testing these pathways will clarify whether the compact morphology observed at HV reflects energy reallocation toward homeostasis, altered resource supply, or additional vent-related constraints.

## 5 Conclusion

Our results indicate that *T. aurea* maintains an elevated $pH_{CF}$ under exceptionally low external pH in a shallow hydrothermal vent environment, with SEM observations revealing no obvious dissolution features in the vent-site skeletons. These findings demonstrate a strong capacity for internal pH regulation, a trait that likely facilitates the persistence of *T. aurea* in highly acidified habitats where most reef-building taxa are absent. Although *T. aurea* is native to our study region and has not been documented as invasive, the persistence of acidification-tolerant taxa could contribute to future shifts in coral community composition if more sensitive reef-building species decline. As global ocean chemistry continues to change, these physiological mechanisms may disproportionately favour such stress-tolerant, non-reef-building taxa, allowing them to expand and dominate ecological niches while placing critical pressure on more vulnerable reef-building corals. Consequently, understanding the trade-off between pH up-regulation and macroscopic growth in resilient native populations is essential for predicting the future structural complexity and ecological trajectory of marine ecosystems.

## Data availability

All data and code needed to evaluate and reproduce the results in the paper are present in the paper and/or the Supplementary Materials. This study did not generate any new materials.

## Author contributions

https://doi.org/10.5194/egusphere-2026-5987
Preprint. Discussion started: 23 October 2026
© Author(s) 2026. CC BY 4.0 License.

Conceptualization: G.K.G., Methodology: G.K.G., L.C.T., Y.I and Y.W.L.; Formal analysis: G.K.G., Writing – original draft: G.K.G.; Writing – review and editing: G.K.G., L.C.T., J.S.H., and Y.W.L.; Supervision: J.S.H., and Y.W.L.; Funding acquisition: J.S.H., and Y.W.L.; Resources: Y.I and Y.W.L.

**Competing interests**

The authors declare they have no competing interests.

**Disclaimer**

Copernicus Publications remains neutral with regard to jurisdictional claims made in the text, published maps, institutional affiliations, or any other geographical representation in this paper. While Copernicus Publications makes every effort to include appropriate place names, the final responsibility lies with the authors. Views expressed in the text are those of the authors and do not necessarily reflect the views of the publisher.

**Acknowledgements**

We gratefully acknowledge the Prince Albert II of Monaco Foundation and the IPCC for their support through the IPCC Scholarship awarded to Gowri Krishna Girija. We extend our sincere thanks to all members of the J.S.H. laboratory for their assistance with field sampling, and to the members of Y.W.L. laboratory for their support with isotopic measurements.

**Financial Support**

This study was supported by the National Science and Technology Council of Taiwan through grants MOST 110-2621-M-019-001, MOST 111-2621-M-019-001 and NSTC 112-2621-M-019-002 to J.S.H., NSTC 112-2116-M-001-034 and NSTC 113-2116-M-001-020 to Y.W.L., and NSTC 114-2621-M-019-003 to L.C.T.

**Review Statement**

**Declaration of generative AI and AI-assisted technologies in the writing process**

The authors did not use any generative AI or AI-assisted technologies for creating content for this work. AI-assisted technologies were used for general editing and grammar check.

**Reference**

https://doi.org/10.5194/egusphere-2026-5987
Preprint. Discussion started: 23 October 2026
© Author(s) 2026. CC BY 4.0 License.

Allison, N. and Finch, A. A.: $\delta^{11}B$, Sr, Mg and B in a modern Porites coral: the relationship between calcification site pH and skeletal chemistry, Geochim. Cosmochim. Acta, 74, 1790–1800, https://doi.org/10.1016/J.GCA.2009.12.030, 2010.

Allison, N., Cole, C., Hintz, C., Hintz, K., Rae, J., and Finch, A.: Resolving the interactions of ocean acidification and temperature on coral calcification media pH, Coral Reefs 2021 406, 40, 1807–1818, https://doi.org/10.1007/s00338-021-02170-2, 2021.

Allison, N., Ross, P., Brasier, A., Cieminska, N., Lopez Martin, N., Cole, C., Hintz, C., Hintz, K., and Finch, A.: Effects of seawater $pCO_2$ on the skeletal morphology of massive Porites spp. corals, Mar. Biol., 169, 1–11, https://doi.org/10.1007/s00227-022-04060-9, 2022.

Allison, N., Venn, A. A., Tambutté, S., Tambutté, E., Wilckens, F. K., Kasemann, S. A., Craven, J., Talavera, C., and de Hoog, C.: A comparison of SNARF-1 and skeletal $\delta^{11}B$ estimates of calcification media pH in tropical coral, Geochim. Cosmochim. Acta, 355, 184–194, https://doi.org/10.1016/J.GCA.2023.07.005, 2023.

Alvarez-Filip, L., Dulvy, N. K., Gill, J. A., Côté, I. M., and Watkinson, A. R.: Flattening of Caribbean coral reefs: Region-wide declines in architectural complexity, Proc. R. Soc. B Biol. Sci., 276, 3019–3025, https://doi.org/10.1098/rspb.2009.0339, 2009.

Anagnostou, E., Huang, K. F., You, C. F., Sikes, E. L., and Sherrell, R. M.: Evaluation of boron isotope ratio as a pH proxy in the deep sea coral *Desmophyllum dianthus*: Evidence of physiological pH adjustment, Earth Planet. Sci. Lett., 349–350, 251–260, https://doi.org/10.1016/J.EPSL.2012.07.006, 2012.

Anthony, K. R. N., Kline, D. I., Diaz-Pulido, G., Dove, S., and Hoegh-Guldberg, O.: Ocean acidification causes bleaching and productivity loss in coral reef builders, Proc. Natl. Acad. Sci. U. S. A., 105, 17442–17446, https://doi.org/10.1073/PNAS.0804478105, 2008.

Bastos, N., Poubel Tunala, L., and Coutinho, R.: Life history strategy of *Tubastraea spp*. corals in an upwelling area on the Southwest Atlantic: Growth, fecundity, settlement, and recruitment, PeerJ, 12, e17829, https://doi.org/10.7717/PEERJ.17829, 2024.

Benavides, M., Bednarz, V. N., and Ferrier-Pagès, C.: Diazotrophs: Overlooked key players within the coral symbiosis and tropical reef ecosystems?, Front. Mar. Sci., 4, 233767, https://doi.org/10.3389/fmars.2017.00010, 2017.

Blain, C. O., Kulins, S., Radford, C. A., Sewell, M. A., and Shears, N. T.: Heterogeneity around $CO_2$ vents obscures the effects of ocean acidification on shallow reef communities, ICES J. Mar. Sci., 78, 3162–3175, https://doi.org/10.1093/icesjms/fsab184, 2021.

Blamart, D., Rollion-Bard, C., Meibom, A., Cuif, J. P., Juillet-Leclerc, A., and Dauphin, Y.: Correlation of boron isotopic composition with ultrastructure in the deep-sea coral *Lophelia pertusa*: Implications for biomineralization and paleo-pH, Geochemistry, Geophys. Geosystems, 8, 12001, https://doi.org/10.1029/2007GC001686, 2007.

Chalk, T. B., Standish, C. D., D'Angelo, C., Castillo, K. D., Milton, J. A., and Foster, G. L.: Mapping coral calcification strategies from in situ boron isotope and trace element measurements of the tropical coral *Siderastrea siderea*, Sci. Reports 2021 111, 11, 1–13, https://doi.org/10.1038/s41598-020-78778-1, 2021.

https://doi.org/10.5194/egusphere-2026-5987
Preprint. Discussion started: 23 October 2026
© Author(s) 2026. CC BY 4.0 License.

Chan, B. K. K., Wang, T. W., Chen, P. C., Lin, C. W., Chan, T. Y., and Tsang, L. M.: Community Structure of Macrobiota and Environmental Parameters in Shallow Water Hydrothermal Vents off Kueishan Island, Taiwan, PLoS One, 11, e0148675, https://doi.org/10.1371/JOURNAL.PONE.0148675, 2016.

Chen, C. T. A., Wang, B. J., Huang, J. F., Lou, J. Y., Kuo, F. W., Tu, Y. Y., and Tsai, H. S.: Investigation into extremely acidic hydrothermal fluids off Kueishan Tao, Taiwan, China, Acta Oceanol. Sin., 125–133, WOS:000228420300013, 2005.

Chen, Y. J., Wu, J. Y., Chen, C. T. A., and Liu, L. L.: Effects of low-pH stress on shell traits of the dove snail, *Anachis misera*, inhabiting shallow-vent environments off Kueishan Islet, Taiwan, Biogeosciences, 12, 2631–2639, https://doi.org/10.5194/BG-12-2631-2015, 2015.

Comeau, S., Cornwall, C. E., and McCulloch, M. T.: Decoupling between the response of coral calcifying fluid pH and calcification to ocean acidification, Sci. Reports 2017 71, 7, 1–10, https://doi.org/10.1038/s41598-017-08003-z, 2017a.

Cornwall, C. E., Comeau, S., Kornder, N. A., Perry, C. T., van Hooidonk, R., DeCarlo, T. M., Pratchett, M. S., Anderson, K. D., Browne, N., Carpenter, R., Diaz-Pulido, G., D'Olivo, J. P., Doo, S. S., Figueiredo, J., Fortunato, S. A. V., Kennedy, E., Lantz, C. A., McCulloch, M. T., González-Rivero, M., Schoepf, V., Smithers, S. G., and Lowe, R. J.: Global declines in coral reef calcium carbonate production under ocean acidification and warming, Proc. Natl. Acad. Sci., 118, e2015265118, https://doi.org/10.1073/PNAS.2015265118, 2021.

Corrigan, E., Chen, C. J., Wang, B. S., Dufour, S., and Chang, C. F.: Robustness of gametogenesis in the scleractinian coral, *Tubastraea aurea*, in the shallow-water hydrothermal vent field off Kueishan Island, northeastern Taiwan, Sci. Total Environ., 992, 179901, https://doi.org/10.1016/J.SCITOTENV.2025.179901, 2025.

Creed, J. C.: Two invasive alien azooxanthellate corals, *Tubastraea coccinea* and *Tubastraea tagusensis*, dominate the native zooxanthellate *Mussismilia hispida* in Brazil, Coral Reefs 2006 253, 25, 350–350, https://doi.org/10.1007/S00338-006-0105-X, 2006.

Crook, E. D., Potts, D., Rebolledo-Vieyra, M., Hernandez, L., and Paytan, A.: Calcifying coral abundance near low-pH springs: Implications for future ocean acidification, Coral Reefs, 31, 239–245, https://doi.org/10.1007/s00338-011-0839-y, 2012.

Doney, S. C., Fabry, V. J., Feely, R. A., and Kleypas, J. A.: Ocean Acidification: The other $CO_2$ problem, https://doi.org/10.1146/annurev.marine.010908.163834, 2009.

Dutra, B. S. V. M., Carlos-Júnior, L. A., and Creed, J. C.: When species become invasive research becomes problem oriented: a synthesis of knowledge of the stony coral *Tubastraea*, Biol. Invasions 2023 257, 25, 2069–2088, https://doi.org/10.1007/S10530-023-03032-4, 2023.

Eagle, R. A., Guillermic, M., De Corte, I., Alvarez Caraveo, B., Bove, C. B., Misra, S., Cameron, L. P., Castillo, K. D., and Ries, J. B.: Physicochemical control of Caribbean coral calcification linked to host and symbiont responses to varying $pCO_2$ and temperature, J. Mar. Sci. Eng., 10, https://doi.org/10.3390/jmse10081075, 2022.

Enochs, I. C., Manzello, D. P., Donham, E. M., Kolodziej, G., Okano, R., Johnston, L., Young, C., Iguel, J., Edwards, C. B., Fox, M. D., Valentino, L., Johnson, S., Benavente, D., Clark, S. J., Carlton, R., Burton, T., Eynaud, Y., and Price, N. N.: Shift from coral to macroalgae dominance on a volcanically acidified reef, Nat. Clim. Chang. 2015 512, 5, 1083–1088,

https://doi.org/10.5194/egusphere-2026-5987
Preprint. Discussion started: 23 October 2026
© Author(s) 2026. CC BY 4.0 License.

https://doi.org/10.1038/nclimate2758, 2015.

Eyre, B. D., Cyronak, T., Drupp, P., De Carlo, E. H., Sachs, J. P., and Andersson, A. J.: Coral reefs will transition to net dissolving before end of century, Science (80-. )., 359, 908–911, https://doi.org/10.1126/SCIENCE.AAO1118, 2018.

Fabricius, K. E., Langdon, C., Uthicke, S., Humphrey, C., Noonan, S., De'ath, G., Okazaki, R., Muehllehner, N., Glas, M. S., and Lough, J. M.: Losers and winners in coral reefs acclimatized to elevated carbon dioxide concentrations, Nat. Clim. Chang., 1, 165–169, https://doi.org/10.1038/NCLIMATE1122, 2011.

Foster, G. L. and Evans, D.: Geochemical constraints on the use of an amorphous precursor phase by corals, Geochemical Perspect. Lett., 40, 56–61, https://doi.org/10.7185/GEOCHEMLET.2623, 2026.

Foster, G. L., Pogge Von Strandmann, P. A. E., and Rae, J. W. B.: Boron and magnesium isotopic composition of seawater, Geochemistry, Geophys. Geosystems, 11, 8015, https://doi.org/10.1029/2010GC003201, 2010.

Gagnon, A. C.: Coral calcification feels the acid, Proc. Natl. Acad. Sci. U. S. A., 110, 1567–1568, https://doi.org/10.1073/PNAS.1221308110, 2013.

Gagnon, A. C., Gothmann, A. M., Branson, O., Rae, J. W. B., and Stewart, J. A.: Controls on boron isotopes in a cold-water coral and the cost of resilience to ocean acidification, Earth Planet. Sci. Lett., 554, 116662, https://doi.org/10.1016/J.EPSL.2020.116662, 2021.

Georgiou, L., Falter, J., Trotter, J., Kline, D. I., Holcomb, M., Dove, S. G., Hoegh-Guldberg, O., and McCulloch, M.: PH homeostasis during coral calcification in a free ocean $CO_2$ enrichment (FOCE) experiment, Heron Island reef flat, Great Barrier Reef, Proc. Natl. Acad. Sci. U. S. A., 112, 13219–13224, https://doi.org/10.1073/PNAS.1505586112, 2015.

Girija, G. K., Tseng, L. C., Chen, Y. L., Meng, P. J., Hwang, J. S., and Ho, Y. N.: Microbiome variability in invasive coral (*Tubastraea aurea*) in response to diverse environmental stressors, Front. Mar. Sci., 10, 1234137, https://doi.org/10.3389/fmars.2023.1234137, 2023.

Girija, G. K., Tseng, L. C., Muthu, P., Chen, Y. L., Ho, Y. N., and Hwang, J. S.: Microbiome flexibility enhances the resilience of the potentially invasive coral *Tubastraea aurea* to abrupt environmental changes: Insights from a shallow water hydrothermal vent transplantation study, Sci. Total Environ., 954, 176792, https://doi.org/10.1016/J.SCITOTENV.2024.176792, 2024.

Guilherme da Silva, A., Carlos-Júnior, L. A., Sasada Sato, C. Y., Lages, B. G., Neres-Lima, V., Sá de Oliveira, F. M., Maia, L. F., Cappa de Oliveira, L. F., and Fleury, B. G.: Living with an enemy: Invasive sun-coral (*Tubastraea spp*.) competing against sponges *Desmapsamma anchorata* in southeastern Brazil, Mar. Environ. Res., 174, 105559, https://doi.org/10.1016/J.MARENVRES.2022.105559, 2022.

Guillermic, M., Cameron, L. P., De Corte, I., Misra, S., Bijma, J., De Beer, D., Reymond, C. E., Westphal, H., Ries, J. B., and Eagle, R. A.: Thermal stress reduces pocilloporid coral resilience to ocean acidification by impairing control over calcifying fluid chemistry, Sci. Adv., 7, https://doi.org/10.1126/SCIADV.ABA9958, 2021.

Gutjahr, M., Bordier, L., Douville, E., Farmer, J., Foster, G. L., Hathorne, E. C., Hönisch, B., Lemarchand, D., Louvat, P., McCulloch, M., Noireaux, J., Pallavicini, N., Rae, J. W. B., Rodushkin, I., Roux, P., Stewart, J. A., Thil, F., and You, C. F.:

https://doi.org/10.5194/egusphere-2026-5987
Preprint. Discussion started: 23 October 2026
© Author(s) 2026. CC BY 4.0 License.

Sub-permil interlaboratory consistency for solution-based boron isotope analyses on marine carbonates, Geostand. Geoanalytical Res., 45, 59–75, https://doi.org/10.1111/GGR.12364, 2021.

Hassenrück, C., Fink, A., Lichtschlag, A., Tegetmeyer, H. E., De Beer, D., and Ramette, A.: Quantification of the effects of ocean acidification on sediment microbial communities in the environment: the importance of ecosystem approaches, FEMS Microbiol. Ecol., 92, https://doi.org/10.1093/femsec/fiw027, 2016.

Hoegh-Guldberg, O., Mumby, P. J., Hooten, A. J., Steneck, R. S., Greenfield, P., Gomez, E., Harvell, C. D., Sale, P. F., Edwards, A. J., Caldeira, K., Knowlton, N., Eakin, C. M., Iglesias-Prieto, R., Muthiga, N., Bradbury, R. H., Dubi, A., and Hatziolos, M. E.: Coral reefs under rapid climate change and ocean acidification., Science, 318, 1737–1742, https://doi.org/10.1126/SCIENCE.1152509, 2007.

Holcomb, M., Venn, A. A., Tambutté, E., Tambutté, S., Allemand, D., Trotter, J., and McCulloch, M.: Coral calcifying fluid pH dictates response to ocean acidification, Sci. Reports 2014 41, 4, 1–4, https://doi.org/10.1038/srep05207, 2014.

Hönisch, B., Hemming, N. G., Grottoli, A. G., Amat, A., Hanson, G. N., and Bijma, J.: Assessing scleractinian corals as recorders for paleo-pH: Empirical calibration and vital effects, Geochim. Cosmochim. Acta, 68, 3675–3685, https://doi.org/10.1016/J.GCA.2004.03.002, 2004.

Houlbrèque, F., Tambutté, E., Richard, C., and Ferrier-Pagès, C.: Importance of a micro-diet for scleractinian corals, Mar. Ecol. Prog. Ser., 282, 151–160, https://doi.org/10.3354/MEPS282151, 2004.

IPCC: Climate Change 2021 – The Physical Science Basis: Working group I contribution to the sixth assessment report of the Intergovernmental Panel on Climate Change, Cambridge University Press, https://doi.org/10.1017/9781009157896, 2023.

Iwagawa, T., Miyazaki, M., Yokogawa, Y., Okamura, H., Nakatani, M., Doe, M., Morimoto, Y., and Takemura, K.: Aplysinopsin dimers from a stony coral. *Tubastraea aurea*, Heterocycles, 75, 2023–2028, https://doi.org/10.3987/COM-08-11358, 2008.

Jeng, M. S., Ngt, N. K., and Ng, P. K. L.: Hydrothermal vent crabs feast on sea 'snow,' Nat. 2004 4327020, 432, 969–969, https://doi.org/10.1038/432969a, 2004.

Jiang, Z. P., Huang, C., Dai, M., Kao, S. J., Hydes, D. J., Chou, W. C., and Janf, S.: Short-term dynamics of oxygen and carbon in productive nearshore shallow seawater systems off Taiwan: Observations and modeling, Limnol. Oceanogr., 56, 1832–1849, https://doi.org/10.4319/LO.2011.56.5.1832, 2011.

Kitahara, M. V., Jaimes-Becerra, A., Gamero-Mora, E., Padilla, G., Doonan, L. B., Ward, M., Marques, A. C., Morandini, A. C., and Long, P. F.: Reciprocal transplantation of the heterotrophic coral *Tubastraea coccinea* (Scleractinia: Dendrophylliidae) between distinct habitats did not alter its venom toxin composition, Ecol. Evol., 10, 1794–1803, https://doi.org/10.1002/ece3.5959, 2020.

Klochko, K., Kaufman, A. J., Yao, W., Byrne, R. H., and Tossell, J. A.: Experimental measurement of boron isotope fractionation in seawater, Earth Planet. Sci. Lett., 248, 276–285, https://doi.org/10.1016/J.EPSL.2006.05.034, 2006.

Krief, S., Hendy, E. J., Fine, M., Yam, R., Meibom, A., Foster, G. L., and Shemesh, A.: Physiological and isotopic responses of scleractinian corals to ocean acidification, Geochim. Cosmochim. Acta, 74, 4988–5001,

https://doi.org/10.5194/egusphere-2026-5987
Preprint. Discussion started: 23 October 2026
© Author(s) 2026. CC BY 4.0 License.

https://doi.org/10.1016/J.GCA.2010.05.023, 2010.

Kubota, K., Yokoyama, Y., Ishikawa, T., Suzuki, A., and Ishii, M.: Rapid decline in pH of coral calcification fluid due to incorporation of anthropogenic $CO_2$, Sci. Reports 2017 71, 7, 1–9, https://doi.org/10.1038/s41598-017-07680-0, 2017.

Lages, B. G., Fleury, B. G., Menegola, C., and Creed, J. C.: Change in tropical rocky shore communities due to an alien coral invasion, Mar. Ecol. Prog. Ser., 438, 85–96, https://doi.org/10.3354/MEPS09290, 2011.

Lages, B. G., Fleury, B. G., Hovell, A. M. C., Rezende, C. M., Pinto, A. C., and Creed, J. C.: Proximity to competitors changes secondary metabolites of non-indigenous cup corals, *Tubastraea spp*., in the southwest Atlantic, Mar. Biol. 2012 1597, 159, 1551–1559, https://doi.org/10.1007/S00227-012-1941-6, 2012.

LASKER, H. R.: Phenotypic variation in the coral *Montastrea cavernosa* and its effects on colony energetics , Biol. Bull., 160, 292–302, https://doi.org/10.2307/1540889, 1981.

Lemarchand, D., Gaillardet, J., Lewin, A., and Allègre, C. J.: Boron isotope systematics in large rivers: implications for the marine boron budget and paleo-pH reconstruction over the Cenozoic, Chem. Geol., 190, 123–140, https://doi.org/10.1016/S0009-2541(02)00114-6, 2002.

Lesser, M. P., Falcón, L. I., Rodríguez-Román, A., Enríquez, S., Hoegh-Guldberg, O., and Iglesias-Prieto, R.: Nitrogen fixation by symbiotic cyanobacteria provides a source of nitrogen for the scleractinian coral *Montastraea cavernosa*, Mar. Ecol. Prog. Ser., 346, 143–152, https://doi.org/10.3354/MEPS07008, 2007.

Lin, Y. S., Lui, H. K., Lee, J., Chen, C. T. A., Burr, G. S., Chou, W. C., and Kuo, F. W.: Fates of vent $CO_2$ and its impact on carbonate chemistry in the shallow-water hydrothermal field offshore Kueishantao Islet, NE Taiwan, Mar. Chem., 210, 1–12, https://doi.org/10.1016/J.MARCHEM.2019.02.002, 2019.

Liu, Y. H., Huang, K. F., and Lee, D. C.: Precise and accurate boron and lithium isotopic determinations for small sample-size geological materials by MC-ICP-MS, J. Anal. At. Spectrom., 33, 846–855, https://doi.org/10.1039/C7JA00400A, 2018.

Liu, Y. W., Sutton, J. N., Ries, J. B., and Eagle, R. A.: Regulation of calcification site pH is a polyphyletic but not always governing response to ocean acidification, Sci. Adv., 6, https://doi.org/10.1126/SCIADV.AAX1314, 2020.

Liu, Y. W., Lin, K., Morgan, K., and Wang, X.: Ocean acidification in the tropical Indian Ocean over the past 37 years: Insights from $\delta^{11}B$ and B/Ca records in a Maldives coral, Chem. Geol., 662, 122243, https://doi.org/10.1016/J.CHEMGEO.2024.122243, 2024.

Mantelatto, M. C. and Creed, J. C.: Non-indigenous sun corals invade mussel beds in Brazil, Mar. Biodivers., 45, 605–606, https://doi.org/10.1007/S12526-014-0282-8, 2015.

McCulloch, M., Falter, J., Trotter, J., and Montagna, P.: Coral resilience to ocean acidification and global warming through pH up-regulation, Nat. Clim. Chang. 2012 28, 2, 623–627, https://doi.org/10.1038/nclimate1473, 2012a.

McCulloch, M., Trotter, J., Montagna, P., Falter, J., Dunbar, R., Freiwald, A., Försterra, G., López Correa, M., Maier, C., Rüggeberg, A., and Taviani, M.: Resilience of cold-water scleractinian corals to ocean acidification: Boron isotopic systematics of pH and saturation state up-regulation, Geochim. Cosmochim. Acta, 87, 21–34, https://doi.org/10.1016/J.GCA.2012.03.027, 2012b.

https://doi.org/10.5194/egusphere-2026-5987
Preprint. Discussion started: 23 October 2026
© Author(s) 2026. CC BY 4.0 License.

Mei, K. ;, Wang, D. ;, Jiang, Y. ;, Shi, M. ;, Chen, C.-T. A. ;, Zhang, Y. ;, Mei, K., Wang, D., Jiang, Y., Shi, M., Chen, C.-T. A., Zhang, Y., and Tang, K.: Transformation, fluxes and impacts of dissolved metals from shallow water hydrothermal vents on nearby ecosystem offshore of Kueishantao (NE Taiwan), Sustain. 2022, Vol. 14, Page 1754, 14, 1754, https://doi.org/10.3390/SU14031754, 2022.

Reynaud, S., Rollion-Bard, C., Martin, S., Rodolpho-Metalpa, R., Gattuso, J. P., & Commission Internationale pour l'Exploration Scientifique de la Mer Mediterranee- CIESM, M.: Effect of elevated $pCO_2$ on the boron isotopic composition into the Mediterranean scleractinian coral *Cladocora caespitosa*, in: In CIESM Workshop . CIESM, Monaco., Monographs (No. 36), https://www.researchgate.net/publication/232707482, 2008.

Reynaud, S., Hemming, N. G., Juillet-Leclerc, A., and Gattuso, J. P.: Effect of $pCO_2$ and temperature on the boron isotopic composition of the zooxanthellate coral *Acropora sp*., Coral Reefs, 23, 539–546, https://doi.org/10.1007/S00338-004-0399-5, 2004.

Roik, A., Wall, M., Dobelmann, M., Nietzer, S., Brefeld, D., Fiesinger, A., Reverter, M., Schupp, P. J., Jackson, M., Rutsch, M., and Strahl, J.: Trade-offs in a reef-building coral after six years of thermal acclimation, Sci. Total Environ., 949, 174589, https://doi.org/10.1016/j.scitotenv.2024.174589, 2024.

Ross, C. L., Falter, J. L., and McCulloch, M. T.: Active modulation of the calcifying fluid carbonate chemistry ($\delta^{11}B$, B/Ca) and seasonally invariant coral calcification at sub-tropical limits, Sci. Reports 2017 71, 7, 1–11, https://doi.org/10.1038/s41598-017-14066-9, 2017.

Scucchia, F., Malik, A., Zaslansky, P., Putnam, H. M., and Mass, T.: Combined responses of primary coral polyps and their algal endosymbionts to decreasing seawater pH, Proc. R. Soc. B, 288, https://doi.org/10.1098/RSPB.2021.0328, 2021.

Tambutté, S., Holcomb, M., Ferrier-Pagès, C., Reynaud, S., Tambutté, É., Zoccola, D., and Allemand, D.: Coral biomineralization: From the gene to the environment, J. Exp. Mar. Bio. Ecol., 408, 58–78, https://doi.org/10.1016/J.JEMBE.2011.07.026, 2011.

Tanaka, K., Holcomb, M., Takahashi, A., Kurihara, H., Asami, R., Shinjo, R., Sowa, K., Rankenburg, K., Watanabe, T., and McCulloch, M.: Response of *Acropora digitifera* to ocean acidification: constraints from $\delta^{11}B$, Sr, Mg, and Ba compositions of aragonitic skeletons cultured under variable seawater pH, Coral Reefs 2015 344, 34, 1139–1149, https://doi.org/10.1007/S00338-015-1319-6, 2015.

Tanasovici, R. M., Dias, G. M., Kitahara, M. V., and Vieira, E. A.: Enduring regardless the conditions: Plasticity in modular growth as a strategy to cope with hydrodynamic variation by the invasive sun-coral (*Tubastraea spp.*), Mar. Environ. Res., 174, 105563, https://doi.org/10.1016/J.MARENVRES.2022.105563, 2022.

Trotter, J., Montagna, P., McCulloch, M., Silenzi, S., Reynaud, S., Mortimer, G., Martin, S., Ferrier-Pagès, C., Gattuso, J. P., and Rodolfo-Metalpa, R.: Quantifying the pH 'vital effect' in the temperate zooxanthellate coral *Cladocora caespitosa*: Validation of the boron seawater pH proxy, Earth Planet. Sci. Lett., 303, 163–173, https://doi.org/10.1016/J.EPSL.2011.01.030, 2011.

Venn, A., Tambutté, E., Holcomb, M., Allemand, D., and Tambutté, S.: Live Tissue Imaging Shows Reef Corals Elevate pH

https://doi.org/10.5194/egusphere-2026-5987
Preprint. Discussion started: 23 October 2026
© Author(s) 2026. CC BY 4.0 License.



under Their Calcifying Tissue Relative to Seawater, PLoS One, 6, e20013, https://doi.org/10.1371/JOURNAL.PONE.0020013, 2011.

Wall, M., Prada, F., Fietzke, J., Caroselli, E., Dubinsky, Z., Brizi, L., Fantazzini, P., Franzellitti, S., Mass, T., Montagna, P., Falini, G., and Goffredo, S.: Linking internal carbonate chemistry regulation and calcification in corals growing at a Mediterranean $CO_2$ vent, Front. Mar. Sci., 6, https://doi.org/10.3389/FMARS.2019.00699, 2019a.

Wall, M., Fietzke, J., Crook, E. D., and Paytan, A.: Using B isotopes and B/Ca in corals from low saturation springs to constrain calcification mechanisms, Nat. Commun. 2019 101, 10, 1–9, https://doi.org/10.1038/s41467-019-11519-9, 2019b.

Wang, C., Yang, M. L., Chou, C. P., Chang, Y. C., and Lee, C. S.: Westward extension of the Okinawa trough at its Western end in the Northern Taiwan area: Bathymetric and seismological evidence, Terr. Atmos. Ocean. Sci., 11, 459–480, https://doi.org/10.3319/TAO.2000.11.2.459(O), 2000.

Zeebe, R. E. and Wolf-Gladrow, D. A.: $CO_2$ in Seawater: Equilibrium, Kinetics, Isotopes, Elsevier Oceanography Series, 65, Elsevier Science, Amsterdam, 346 pp., ISBN: 0444509461, 2001.

Zeng, Z., Wang, X., Chen, C. T. A., Yin, X., Chen, S., Ma, Y., and Xiao, Y.: Boron isotope compositions of fluids and plumes from the Kueishantao hydrothermal field off northeastern Taiwan: Implications for fluid origin and hydrothermal processes, Mar. Chem., 157, 59–66, https://doi.org/10.1016/J.MARCHEM.2013.09.001, 2013.